ELSEVIER

Chemical Geology 199 (2003) 71–82

CHEMICAL GEOLOGY
INCLUDING
ISOTOPE GEOSCIENCE

www.elsevier.com/locate/chemgeo

Environmental arsenopyrite stability and dissolution: theory, experiment, and field observations

D. Craw*, D. Falconer, J.H. Youngson

Geology Department, University of Otago, Leith Street, PO Box 56, Dunedin 9001, New Zealand

Received 29 August 2002; accepted 13 February 2003

Abstract

Arsenopyrite has traditionally been considered to be chemically unstable in the surficial environment. However, field evidence demonstrates that arsenopyrite does not readily decompose under water-saturated near-surface conditions. Arsenopyrite occurs in the heavy mineral suite of a variety of thin sediments in southern New Zealand, with no evidence for chemical corrosion. These sediments have been water-saturated but within metres of the surface for 10, 60, 28 000, and >2 million years. These observations of long-term arsenopyrite stability are in accord with geochemical predictions based on recent experimentally determined thermodynamic data for arsenopyrite. Calculations using the new thermodynamic data suggest that arsenopyrite has similar Eh–pH stability range to pyrite, except under acid conditions ($pH < 4$) where arsenopyrite should transform to realgar or orpiment. Calculated As concentrations in equilibrium with the pyrite–arsenopyrite assemblage in the surficial environment are 0.01–0.1 ppm, similar to groundwater in arsenopyrite-bearing rocks in this study (0.005–0.3 ppm), and these waters may be in chemical equilibrium. Arsenopyrite decomposes in oxidised waters to yield up to 1100 ppm dissolved As in the laboratory and up to 400 ppm dissolved As in mine processing waters. These concentrations of dissolved As are several orders of magnitude lower than equilibrium solubility of arsenopyrite because of kinetic effects and development of protective oxide coatings on arsenopyrite grains. Mine tailings containing arsenopyrite should be chemically stable during long-term storage provided they are kept water-saturated and moderately reduced.

Keywords: Arsenopyrite; Solubility; Thermodynamic data; Detrital minerals; Arsenic; Mine tailings

1. Introduction

Arsenic is one of the so-called heavy metals (metalloids) which is toxic in the environment at low concentrations (parts per billion, ppb, levels). The most common natural occurrences of arsenic are associated with hydrothermal gold deposits and these are further exposed by mining and processing. Arsenic-rich discharges are well known from gold mine tailings, but also there is less spectacular As release during weathering and groundwater interaction with arsenic-rich rocks, contributing to background or natural elevation of dissolved arsenic concentrations (Smedley and Kinniburgh, 2002).

Arsenopyrite, FeAsS, is the dominant arsenic mineral in most As-bearing natural occurrences and is therefore the mineral most commonly implicated at

---

* Corresponding author. Tel.: +64-3-4797519; fax: +64-3-4797527.

E-mail address: dave.craw@stonebow.otago.ac.nz (D. Craw).

0009-2541/03/$ - see front matter © 2003 Elsevier Science B.V. All rights reserved.
doi:10.1016/S0009-2541(03)00117-7

surface sites with elevated arsenic concentrations (Smedley et al., 1996). Detailed laboratory studies (Richardson and Vaughan, 1989; Nesbitt and Muir, 1998) have elucidated the mineral surface decomposition mechanisms associated with this arsenopyrite oxidation. However, despite the common occurrence and environmental significance of arsenopyrite, little is known of the stability, and geochemical decomposition reactions, of arsenopyrite in natural and anthropogenic settings. This study uses observations from field sites and simple laboratory experiments to obtain information on arsenopyrite stability in the surficial environment. We then relate these observations to new geochemical data on arsenopyrite (Pokrovski et al., 2002) to develop a theoretical description of arsenopyrite stability under surficial conditions.

2. Field observations

Field observations for this study focus on natural and mined occurrences in Otago Schist, New Zealand (Fig. 1), where uniform hydrothermal vein mineralogy and host rock composition over a large area, and long mining history, provide many contrasting arsenopyrite occurrences. This schist belt consists of Mesozoic metasediments which were exhumed in the Cretaceous. Tertiary–recent tectonics have caused localised

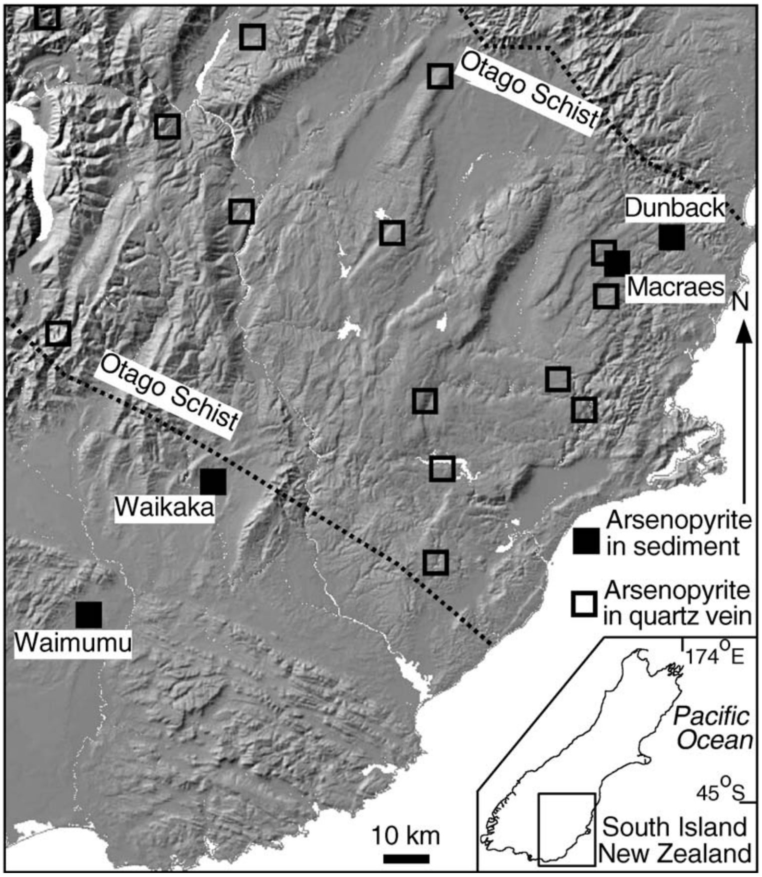

Fig. 1. Sketch geological map of the southern South Island of New Zealand (see inset for location), based on a digital elevation model (www.Geographx.co.nz). Basement rocks form ridges and uplands, and host arsenopyrite-bearing quartz veins (open squares). Sediments derived from basement uplands since the Miocene have accumulated in topographic low relief areas, and some sediments contain arsenopyrite (filled squares).

uplift of the schist belt, as shown by topographic high areas in Fig. 1. Intervening low relief areas in Fig. 1 have received sediment eroded from the schist uplands. We describe arsenopyrite occurrences in veins in the schist basement, and in sediments derived from that basement by natural and mining processes.

2.1. Gold-bearing quartz veins

Arsenopyrite occurs as an important component (typically 1–2%) of gold-bearing quartz veins in the Otago Schist (Fig. 4; Williams, 1974). The arsenopyrite is commonly coarse-grained (typically 1 mm) and enclosed in quartz or impregnating schist breccia fragments within and adjacent to the quartz veins. The arsenopyrite is generally intimately intergrown with pyrite, and minor amounts of other sulphides: sphalerite, galena, chalcopyrite, and stibnite. These sulphide intergrowths contain gold as 1–500 μm grains in fractures, along sulphide grain boundaries, and totally enclosed in individual sulphide grains. The veins range from 1 cm to 5 m in width, and can be traced laterally for 2–100 m. Pyrite has been locally remobilised on to nearby joints by groundwater, but no arsenopyrite has been observed in these joint coatings. Veins, pyritic joints, and enclosing schist have been variably weathered and oxidized for up to 10 m below the present topographic surface. The host schist contains sufficient calcite to neutralize any acidification from oxidation of sulphide minerals, and pH of associated waters range between 5.5 and 8.

Veins have been mined sporadically for gold or scheelite over the past 130 years, and small-scale abandoned workings are widespread (Craw et al., 2000). A prominent zone of veins is currently being mined for gold near Macraes (Fig. 1), where open pits are exposing arsenopyrite-bearing rock up to 100 m below surface. The ore is crushed finely (ca 15 μm) and processed by carbon-in-pulp cyanidation at pH>10, and tailings are discharged into impoundments retained behind earth dams.

Arsenopyrite occurs in a wide range of near-surface situations, as listed in Table 1. Water in contact with this arsenopyrite causes some decomposition and dissolution of arsenic, at a wide range of concentrations. Sampling and analysis of these waters has been described by Craw et al. (1999, 2000) and Craw and Pacheco (2002), and the data are summarised in Table 1 in the context of arsenopyrite decomposition. Arsenopyrite in fresh rocks exposed in mines and drillcore is white and shiny with no obvious surface coating. Arsenopyrite grains in incipiently weathered rocks within ca. 10 m of the surface have a faint yellow-brown tarnish. This tarnish gives way to iron oxyhydroxide coatings as intensity of weathering increases towards the surface. Mineralised rocks exposed at the surface have most arsenopyrite replaced by iron oxyhydroxide and scorodite, but relict variably tarnished grains are preserved in the centres of some quartz veins.

Natural groundwaters in contact with arsenopyrite typically have dissolved As below 0.005 ppm, although groundwater emanating from historic mines has dissolved As up to 4 ppm (Table 1). Rainwater runoff in freshly exposed mine rocks can reach 0.25 ppm within hours of precipitation, and 0.7 ppm within weeks (Table 1). Pore water in contact with fresh arsenopyrite in mine tailings has less than 3 ppm dissolved As after up to 5 years (Craw and Pacheco, 2002). However, agitation and oxidation of arsenopyrite in the processing plant at Macraes can result in dissolved As concentrations up to 400 ppm, dropping to 20–40 ppm in process water sitting on tailings (Table 2). Most dissolved arsenic in surficial settings is As(V), but appreciable As(III) can survive from arsenopyrite decomposition immediately beneath the surface (Table 1; Craw and Pacheco, 2002). All oxidized settings in which arsenopyrite is dissolving have associated iron oxyhydroxide as a precipitate or as suspended fine-grained particulate matter in waters.

2.2. Arsenopyrite in sediments

Sediments derived by erosion, including mining, of mineralised quartz veins in the Otago Schist contain arsenopyrite at several localities (Fig. 1). These localities are described in the following paragraphs in order of increasing age. The youngest such sedimentary deposit is the tailings derived from the Macraes mine. Sulphide-rich tailings, containing pyrite and arsenopyrite, were deposited immediately after the mine opened in 1990. These are currently (2001–2003) being reprocessed, allowing examination of the early tailings deposits, ca. 10 years old. These tailings have

Table 1
Summary of arsenic contents of Otago Schist rock and associated waters in contact with that rock for various time scales

	Setting	Situation	Minerals	Asp texture	Time scale	pH (range)	As in rock (range)	As in water (range)	As species	Eh (mV) (range)	Representative water analyses (ppm)								
											Na	K	Ca	Mg	Cl	HCO_3	SO_4	pH	As
Oxidized rock	Groundwater near historic mine workings	oxidized rock, unmineralised	schist, clays, HFO	none present	10's to 100's of years	5–8	2–6 ppm	<0.001 ppm	nd	0 to +300	13	2	10	5	9	81	4	6.7	<0.005
											52	4	93	20	15	195	226	5.1	<0.005
		oxidized rock, mineralised (mines)	schist, clays, HFO, scor, py, asp	largely altered	10's to 100's of years	6–7.5	2 ppm—2%	0.5–4 ppm	As(V)> As(III)	0 to +300	19	2	135	32	12	427	158	7.0	2
											25	7	125	28	12	400	121	6.9	4.1
Fresh rock		Fresh rock, unmineralised	schist	none present	10's to 100's of years	7–8	2–6 ppm	0.001–0.01 ppm	nd	− 200 (estimate)	12	1	56	10	6	229	6	7.4	0.008
											10	1	3	5	8	58	4	7.4	<0.005
		Fresh rock, mineralised	schist, asp, py, cc	no visible alteration	10's to 100's of years	6.5–8.5	2 ppm—2%	0.005–0.1 ppm	As(III)	− 200 (estimate)	102	6	180	43	49	327	534	6.6	0.044
											42	2	887	30	19	410	24	7.4	0.058
	Surface water	Fresh rock, unmineralised	schist	none present	weeks	7.5–8.5	2–6 ppm	<0.010 ppm	nd	0 to +200	10	1	9	3	14	40	6	8.3	<0.005
											10	3	16	5	12	67	17	6.9	0.006
		Fresh rock, mineralised	schist, asp, py, cc	rare faint yellow tarnish	hours to weeks	7.5–8.5	2 ppm—2%	0.04–0.7 ppm	As(V)> As(III)	0 to +200	21	4	96	74	9	237	317	8.2	0.366
											20	7	133	36	4	179	378	7.7	0.17
Mining process	Cyanidation plant (Macraes mine)	moving crushed rock slurry	schist, asp, py, cc	no visible alteration	days	10.4	up to 5%	25–400 ppm	As(V)> As(III)	nd	nd	nd	nd	nd	nd	nd	nd	10.4	260
											nd	nd	nd	nd	nd	nd	nd	10.4	404
	Tailings dam (Macraes mine)	fresh tailings	schist, asp, py, cc	no visible alteration	months to 4 years	8–10	up to 5%	25–250 ppm	As(III)> As(V)	− 200 to + 50	nd	nd	nd	nd	nd	nd	416	10.1	148
											nd	nd	nd	nd	nd	nd	620	9.3	153
		water on old tailings			5 years	8–8.5	up to 5%	20–40 ppm	As(V)> As(III)	− 150 to + 100	5	50	50	16	155	230	880	8.2	20
											298	31	31	6	84	163	550	8.3	32

Compiled from Craw et al. (1999, 2000) and Craw and Pacheco (2002). Abbreviations: qtz = quartz; asp = arsenopyrite; py = pyrite; scor = scorodite; cc = calcite; HFO = Fe oxyhydroxide; nd = not determined. Schist minerals: quartz, albite, muscovite, chlorite, epidote, titanite, calcite, pyrite, and graphite.

Table 2
Results of experimental dissolution of arsenopyrite with indicated grain sizes, in unsealed (A) and sealed (B) containers (see text)

(A) Arsenopyrite in water, unsealed

Size (μm)	Starting pH	Time (days)	As, ppm	Final pH	Final Eh (mV)
< 180	3.0	7	780	3.9	473
< 180	3.0	28	740	4.2	450
< 180	3.0	56	900	4.3	450
< 180	3.0	84	1053	4.5	430
< 180	3.0	180	145	3.0	520
< 180	3.0	365	645	3.0	522
< 180	5.0	7	580	4.4	445
< 180	5.0	28	756	4.3	435
< 180	5.0	56	886	4.4	440
< 180	5.0	84	887	4.5	430
< 180	5.0	180	145	3.0	526
< 180	5.0	365	607	3.0	512
< 180	7.0	7	260	7.1	275
< 180	7.0	28	321	8.5	202
< 180	7.0	56	361	8.0	226
< 180	7.0	84	403	7.9	241
< 180	7.0	180	198	2.7	548
< 180	7.0	365	651	2.9	534
< 180	9.0	7	350	8.5	201
< 180	9.0	28	425	8.5	205
< 180	9.0	56	490	8.1	234
< 180	9.0	84	469	8.3	202
< 180	9.0	180	46	3.8	470
< 180	9.0	365	388	3.7	480
300–500	3.0	180	302	2.9	523
300–500	3.0	365	477	3.0	516
300–500	5.0	180	186	3.4	492
300–500	5.0	365	436	3.3	516
300–500	7.0	180	100	3.3	508
300–500	7.0	365	127	5.8	350
300–500	9.0	180	154	7.5	256
300–500	9.0	365	137	5.0	405
>1000	3.0	180	157	3.0	521
>1000	3.0	365	379	3.0	534
>1000	5.0	180	175	3.0	516
>1000	5.0	365	403	3.1	530
>1000	7.0	180	70	7.0	280
>1000	7.0	365	129	8.4	198
>1000	9.0	180	96	8.4	200
>1000	9.0	365	174	5.7	369

(B) Arsenopyrite in water, sealed

Size (μm)	Starting pH	Time (days)	As, ppm	Final pH	Final Eh (mV)
< 180	3.0	7	180	3.6	421
< 180	3.0	28	258	3.9	410
< 180	3.0	56	313	4.2	380
< 180	3.0	84	341	4.6	380
< 180	3.0	180	31	4.3	405
< 180	3.0	365	51	4.5	382
< 180	3.0	730	41.8	4.4	371
< 180	5.0	7	137	4.7	358
< 180	5.0	28	230	4.9	341
< 180	5.0	56	268	4.8	362
< 180	5.0	84	266	5.0	341
< 180	5.0	180	19	4.4	375
< 180	5.0	365	41	4.4	391
< 180	5.0	730	60.5	4.6	372
< 180	7.0	7	104	6.8	240
< 180	7.0	28	122	6.8	229
< 180	7.0	56	191	6.6	251
< 180	7.0	84	189	6.5	239
< 180	7.0	180	10	4.4	376
< 180	7.0	365	29	6.9	226
< 180	7.0	730	60.8	4.4	392
< 180	9.0	7	94	8.3	143
< 180	9.0	28	151	8.0	163
< 180	9.0	56	189	8.2	150
< 180	9.0	84	193	8.0	171
< 180	9.0	180	10	6.5	260
< 180	9.0	365	19	7.1	226
< 180	9.0	730	44.8	7.6	195
300–500	3.0	180	48	3.7	420
300–500	3.0	365	22	4.6	370
300–500	3.0	730	68.7	4.0	410
300–500	5.0	180	28	4.3	373
300–500	5.0	365	37	4.9	350
300–500	5.0	730	59.5	4.1	420
300–500	7.0	180	31	6.3	270
300–500	7.0	365	36	6.1	281
300–500	7.0	730	24	4.7	358
300–500	9.0	180	36	6.9	229
300–500	9.0	365	46	6.9	230
300–500	9.0	730	30.8	7.7	171
>1000	3.0	180	26	4.2	405
>1000	3.0	365	34	5.1	340
>1000	3.0	730	46.3	4.1	406
>1000	5.0	180	26	3.7	432
>1000	5.0	365	36	5.7	310
>1000	5.0	730	27.8	4.0	421
>1000	7.0	180	16	6.2	256
>1000	7.0	365	26	7.7	174
>1000	7.0	730	42.2	8.3	150
>1000	9.0	180	32	7.9	167
>1000	9.0	365	41	8.3	148
>1000	9.0	730	30.4	8.0	170

remained saturated with water since deposition, and still have their original depositional pH of ca. 10. Arsenopyrite in these tailings show no signs of tarnish or surface alteration, and are identical in shape, texture, and grain size with arsenopyrite samples obtained from the processing plant in the early stages of mining. Similar observations were reported on the tailings, when 5 years old, by Craw et al. (1999).

Historic mine tailings from the Macraes area were discharged into the nearest stream, and remnants of these tailings can be found in the active stream near Dunback (Fig. 1), ca. 40 km downstream from the mines. This tailing disposal practice ceased about 1940. Rare arsenopyrite grains from these mine tailings occur in bedrock crevices and in basal lags in the gravel-dominated stream bed. The arsenopyrite grains are irregular in shape, but have sharp edges, perfectly preserved striations, and flat crystal faces, as shown in electron-optical images (Fig. 2A). Grains show little evidence of rounding, although some corners are fractured, and there is no evidence of chemical corrosion after submergence for more than 60 years. The arsenopyrite is accompanied by pyrite from the mine tailings, as well as authigenic pyrite eroded from nearby Tertiary marginal marine sediments.

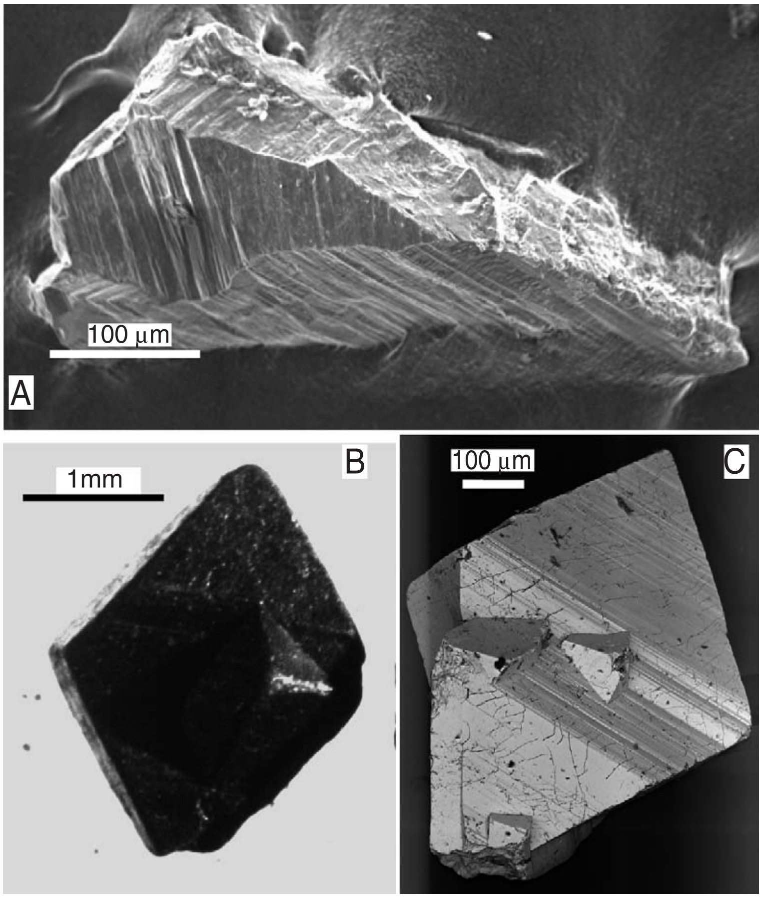

Fig. 2. Arsenopyrite grains from sediments at localities indicated in Fig. 1. (A) Scanning electron microscope image of an arsenoprite grain from a basement crevice in an active stream, ultimately derived from >60-year-old mine tailings discharged into a stream at Macraes. (B) Photograph of a large detrital arsenopyrite grain from 28 000-year-old sediments at Macraes. (C) Scanning electron microscope image of an arsenoprite grain from gold-bearing Miocene–Pliocene sediments at Waimumu.

Proximal sediments derived by erosion of mineralised rocks on a Quaternary fault scarp at Macraes (Fig. 1) contain abundant arsenopyrite and pyrite (Craw and Chappell, 1999). Grains commonly consist of euhedral crystals that range from micron to millimetre scale. The coarser grains are partially rounded on crystal corners (Fig. 2B), but light and electron microscopies yield no textural evidence for chemical alteration The enclosing sediments are up to 28 000 years old, but have remained within 5 m of the surface throughout that time (Craw and Chappell, 1999). Authigenic pyrite has formed in organic-rich portions of the sedimentary pile, in close proximity to the detrital pyrite and arsenopyrite grains.

Miocene–Pliocene fluvial sediments derived from the Otago Schist underlie most of the low-lying areas to the south of the schist belt (Fig. 1). Some parts of this sedimentary sequence have been reworked by fluvial processes after initial deposition. Arsenopyrite grains have been found in the auriferous heavy mineral suite of these sediments at two gold-mining localities, Waikaka and Waimumu (Fig. 1). The arsenopyrite grains are generally small (hundreds of microns), have little evidence of rounding, and no evidence of chemical corrosion (Fig. 2C). The sediments contain detrital pyrite, and are locally cemented by authigenic pyrite and/or marcasite that are accompanied by authigenic gold (Clough and Craw, 1989), but no textural evidence for authigenic arsenopyrite has been found. Formation water becomes acidified by pyrite oxidation when these sediments are exposed to the atmosphere by erosion or mine cuts.

3. Laboratory experiments

Dissolution of sparingly soluble minerals in the surficial environment is commonly incomplete and equilibrium is rare. Hence, a set of simple laboratory experiments was set up to examine the extent of arsenopyrite dissolution under a range of situations representative of the natural and mining environment. These experiments were not intended to be a rigorous evaluation of the equilibrium solubility of arsenopyrite, but rather to obtain an estimate of the amount of decomposition arsenopyrite is likely to undergo under surficial conditions of the type described in the field settings above.

The experiments were run at pH of 3, 5, 7, and 9, for test tubes open to the atmosphere, and for test tubes covered with screw-top lids and sticky tape to restrict oxygen access. Arsenopyrite charges with grain sizes of <180 μm, 300–500 μm, and 1–2 mm (selected by sieving) were used for each set of conditions. About 10 g of sieved crushed material from originally coarse-grained arsenopyrite from Deloro, Ontario, supplied by Wards Scientific was used for each charge. Ten millilitres of water was added to experiments run in unsealed tubes with screw tops, and this was topped up periodically as water evaporated. Thirty millilitres of water was added to the covered experiments. Initial solution pH was controlled with sulphuric acid or 1 M NaOH. Sets of these experiments were run for 1, 4, 8, and 12 weeks, and 6, 12, and 24 months. After the appointed time, the supernatant fluid was extracted by pipette after ensuring that all particulate material had settled on the bottom. Solutions were then acidified and analysed for As by inductively coupled plasma mass spectrometry. Redox potential and final pH were measured with an Oakton WD-35615-series pH/mV/°C meter. Selected arsenopyrite experimental charges were examined by incident light microscopy and electron microscopy to search for evidence of coating by secondary minerals or dissolution. No evidence of either process was seen, but a micron-scale coating of a yellow-brown precipitate developed by evaporation on the walls of some of the open glass tubes immediately above water level.

Results of these experiments are presented in Table 2. The Eh of all final solutions was moderately oxidized, between $+0.15$ and $+0.6$ V. Final pH of most of the reaction tubes was within 2 pH units of the initial pH, with some being more acid and some more alkaline (Table 2). Some of the neutral and alkaline experiments underwent more extreme acidification (Table 2), but these included some of the lower dissolved arsenic tubes (<400 ppm).

The highest dissolved As concentrations occurred in acid unsealed tubes with finest-grained arsenopyrite, and the lowest concentrations were for coarse-grained charges in sealed alkaline tubes (Table 2; Fig. 3A). However, there is considerable overlap of results over the wide range of conditions examined. The highest dissolved As concentrations were in tubes

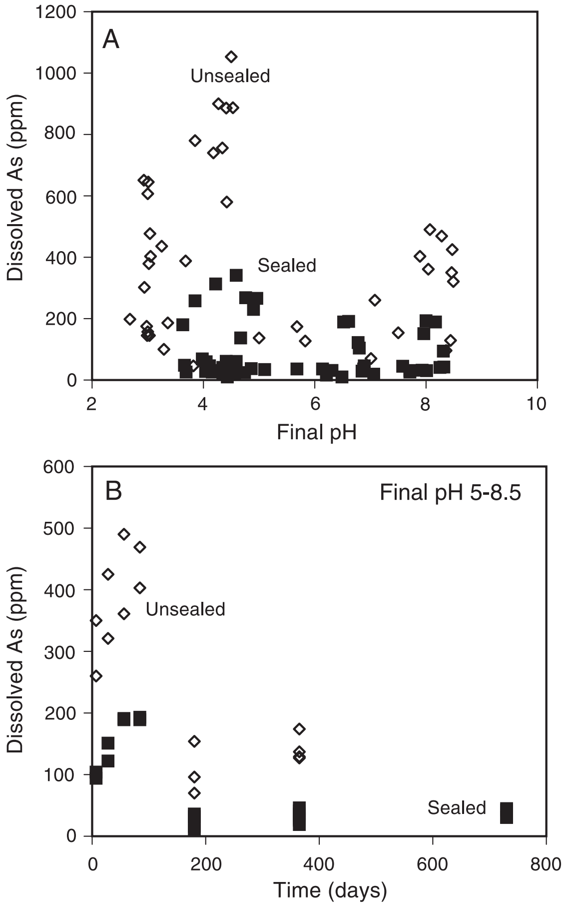

Fig. 3. Results of laboratory experiments which quantify degrees of decomposition of various grain sizes of arsenopyrite in water at a range of pH and times up to 2 years (see text and Table 2) at room temperature (ca. 18 °C) and pressure. (A) Dissolved As concentrations in water at the end of the experiments, as a function of final pH of the solutions. Unsealed experiments are shown as open diamonds, and sealed experiments are black squares. (B) Dissolved As concentration as a function of time for experiments with final pH between 5 and 8.5, the pH range of most significance to this study (Table 1). Symbols are the same as in A.

kept for less than 1 year, and some tubes attained several hundred ppm dissolved As after only 1 month (Table 2). The tubes kept sealed had generally lower dissolved As (< 400 ppm) than the unsealed tubes, although there was considerable overlap of data. For the pH range of most interest in this study, pH 5–8.5, the highest dissolved As (up to 500 ppm) developed in the first few months in unsealed tubes, and tubes kept longer had lower dissolved As (< 100 ppm; Fig. 3B). Sealed tubes showed a similar but more subdued pattern of early elevated As and later lower As contents (Fig. 3B).

4. Theoretical stability of arsenopyrite

4.1. Calculation of Eh–pH diagrams

Most studies of arsenopyrite stability have focussed on high temperature hydrothermal situations (Barton, 1969; Kretschmar and Scott, 1976; Heinrich and Eadington, 1986; Pokrovski et al., 2002). From studies such as these, estimates of the thermodynamic properties of arsenopyrite have been made, and tabulated (e.g., Naumov et al., 1974; Wagman et al., 1982). These data form the basis of predictive stability calculations for arsenopyrite under surficial conditions. Most such calculations suggested that arsenopyrite is not stable in the surficial environment, or that it is stable under extreme conditions not normally encountered (e.g., Vink, 1996; Fig. 4A).

Recent experimental work by Pokrovski et al. (2002) has demonstrated that $\Delta G_{298}{}^{\circ}$ for arsenopyrite is -141.6 ± 6 kJ/mol, at least 30 kJ/mol lower than previous estimates. This new value for $\Delta G_{298}{}^{\circ}$ allows recalculation of arsenopyrite stability under surficial conditions, and the results (Fig. 4A,B) show that arsenopyrite should be considerably more stable in the surficial environment than was previously thought. The lower parts of these diagrams have been calculated using the thermodynamic data compiled in Table 3, and the upper parts of the diagrams have been summarised from Vink (1996). The upper parts of the diagrams are only superficially relevant to this study. Amorphous $Fe(OH)_3$ is used in the diagram because this material is common in natural settings (above), rather than more thermodynamically stable hematite. The diagrams were calculated for relatively dilute groundwater in arsenopyrite-bearing rocks (Fig. 4A), and for mine waters with slightly elevated Fe and As and strongly elevated dissolved sulphur (Fig. 4B). There are few differences in the stability fields of arsenopyrite in these two diagrams.

The most notable feature of the diagrams in Fig. 4 is the large field of stability of arsenopyrite

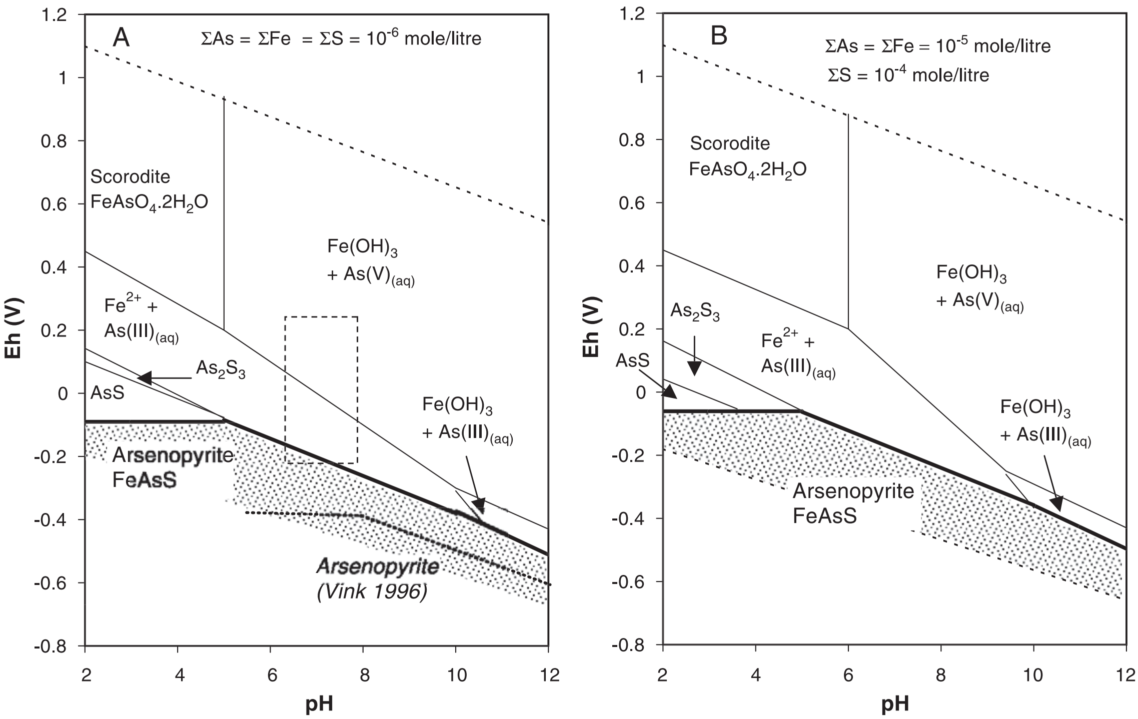

Fig. 4. Eh–pH diagrams (25 °C, 1 atm) for the As–Fe–O–S system showing the stability field of arsenopyrite (stippled; heavy lines) calculated using new thermodynamic data from Pokrovski et al. (1996, 2002) (Table 3). Upper parts of the diagrams are summarised, for clarity, from Vink (1996). Dashed box in the centre of each diagram shows typical near-surface conditions, as summarised in Table 1. (A) Diagram calculated for dissolved As, Fe, and S of 10^{-6} mol/l. Stability field for arsenopyrite from Vink (1996), calculated using old thermodynamic data, is shown with dotted lines. (B) Diagram calculated for dissolved As and Fe of 10^{-5} mol/l and S of 10^{-4} mol/l.

compared to the other arsenic sulphides, orpiment (As_2S_3) and realgar (AsS). One or both of the latter two sulphides are stable over a wide range of pH (0–12) in an iron-free environment (as summarised by Webster, 1990; Vink, 1996). Addition of iron to the system caused little change to the predicted stability ranges of these sulphides if the old thermodynamic data were used, but the new data suggest that orpiment and realgar replace arsenopyrite only under acid conditions (Fig. 4A,B). Thermodynamic data for orpiment and realgar in Fig. 4A and B were taken from Pokrovski et al. (1996) for consistency with the arsenopyrite data used (Table 2), but use of thermodynamic data from, e.g., Webster (1990) has only minor effects on the geometry of the diagrams.

Table 3

Thermodynamic data used to calculate the stability of arsenopyrite in Fig. 4A and B

Compound		ΔG°_{298} (kJ/mol)	Source
FeAsS	arsenopyrite	– 141.6	1
AsS	realgar	– 33.2	2
As_2S_3	orpiment	– 86.0	2
H_3AsO_3	aqueous species	– 639.8	2
$H_2AsO_3^-$	aqueous species	– 587.1	3
Fe^{2+}	aqueous species	– 91.5	3
$Fe(OH)_3$	iron oxyhydroxide	– 696.3	4
Fe_3O_4	magnetite	– 1015.5	4
HS^-	aqueous species	12.0	3
SO_4^{2-}	aqueous species	– 744.5	3
H_2S	aqueous species	– 27.6	4

Sources: (1) Pokrovski et al. (2002); (2) Pokrovski et al. (1996); (3) Shock and Helgeson (1988); (4) Wagman et al. (1982).

4.2. Theoretical solubility

The reaction in Fig. 4A and B that has most significance to arsenopyrite decomposition in the surficial environment is that which yields Fe^{2+}(aq) and a dissolved As(III) species. This reaction occurs over a wide pH range, from ca. 4 to 10. The exact As(III) species varies with pH, but $H_3AsO_3(aq)$ has the widest stability ($pH < 9$; Vink, 1996). The arsenopyrite decomposition reaction is:

$$FeAsS + 7H_2O = Fe^{2+}(aq) + H_3AsO_3(aq) + 11H^+ + 11e^- + SO_4^{2-} \quad (1)$$

The theoretical solubility of arsenopyrite can be calculated from this equation and the data in Table 3, for given pH and Eh conditions. Solubility predictions for the solution concentrations in Fig. 1A are depicted in Fig. 5. Very small changes in redox potential result in large changes in theoretical solubility for any given pH. Arsenopyrite becomes extremely soluble immediately on the oxidized side of the stability boundaries drawn in Fig. 4A and B, with equilibrium dissolved As predicted to rise to thousands of ppm over < 100 mV redox rise (Fig. 5). Conversely, arsenopyrite is extremely insoluble (dissolved As $< 10^{-5}$ ppm) under redox conditions < 100 mV below the stability boundaries in Fig. 4A and B.

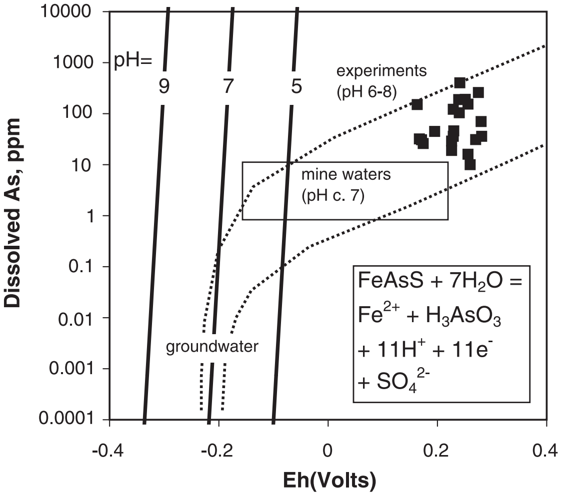

Fig. 5. Predicted solubility of arsenopyrite (heavy lines) calculated from Eq. (1) using thermodynamic data in Table 3 (see text), as a function of Eh and pH at 25 °C and 1 atm pressure. Dotted lines show the inferred range in dissolved arsenic concentrations, based on field observations of mine waters (open box; Table 1) and experiments for pH near 7 (black squares; Table 2).

5. Discussion and conclusions

Theoretical calculations, based on new thermodynamic data (Pokrovski et al., 2002), show that arsenopyrite is more chemically stable under near-surface conditions than was previously thought. The arsenopyrite stability field (Fig. 4A,B) is almost as broad as that for pyrite in Eh–pH space (Garrels and Christ, 1965). The upper (redox) stability boundary for both arsenopyrite and pyrite is close to the H_2S/SO_4^{2-} equal concentration boundary (Garrels and Christ, 1965). Below this boundary, arsenopyrite is extremely insoluble and can remain chemically stable on geological time scales. Consequently, arsenopyrite and pyrite can be expected to coexist with negligible decomposition under moderately reducing surficial conditions. The field evidence (above) of preservation of chemically unaltered arsenopyrite with pyrite under water-saturated surficial conditions for 10, 60, 28 000, and >2 million years supports this new thermodynamic data.

Previous thermodynamic data predicted that realgar and/or orpiment should replace arsenopyrite under reducing surficial conditions, although no geological evidence for this replacement has been reported. The new thermodynamic data suggest that realgar and orpiment should replace arsenopyrite only under acidic conditions ($pH < 4$; Fig. 4A,B). This is consistent with field observations that in reducing environments where pH>5, arsenopyrite does not alter to these other sulphides. The newly defined stability range for arsenopyrite gives credence to suggestions that authigenic arsenopyrite could form naturally in the surficial environment to sequester arsenic (Rittle et al., 1995), rather than orpiment or realgar.

The maximum observed dissolved As (Fig. 3A) of ca. 1100 ppm at pH 3 and Eh of ca. 0.4 V is many orders of magnitude lower than the theoretical solubility of arsenopyrite (Fig. 5). Hence, geochemical equilibrium was not approached for any of the laboratory experiments on a time scale of up to 2 years. This disequilibrium persistence of arsenopyrite is probably due to formation of a submicron-scale protective oxide layer on grain surfaces, including iron oxyhydroxide and scorodite-like material (Richardson and Vaughan, 1989; Nesbitt and Muir, 1998). The apparent decrease in dissolved As with time in the laboratory experiments of this study (Table 2; Fig. 3B) is consistent with such formation of a submicron protective oxidized coating on arsenopyrite, probably accompanied by precipitation and/or adsorption of previously dissolved As. Formation of this protective oxide coating in natural settings may ensure that arsenopyrite can survive water dissolution during sedimentary transport in rivers for tens or hundreds of kilometres (Fig. 2A,C).

Extensive agitation and induced oxidation of arsenopyrite in the Macraes mineral processing plant causes dissolved As to rise to 400 ppm on a time scale of days at a pH near 10 (Table 1). The redox potential of these waters has not been measured, but both As(V) and As(III) are present with As(V) dominant (Craw and Pacheco, 2002). The As speciation implies that Eh is at least 100 mV higher than that of the arsenopyrite stability field boundary (Fig. 4B). Predicted solubility of arsenopyrite under these conditions is several orders of magnitude higher than the observed 400 ppm maximum. Again, protective oxide layers may explain the limited dissolution of this finely comminuted (ca. 15 μm) arsenopyrite. Short-term contact (hours to weeks) between water and arsenopyrite in fresh mine open cuts results in < 1 ppm dissolved As, many orders of magnitude below predicted solubility, presumably because of kinetic factors. Under highly oxidizing conditions, dissolved arsenic concentrations may be related to solubility of scorodite, rather than that of arsenopyrite (Fig. 4A,B; Vink, 1996).

The stoichiometry of Eq. (1) suggests that arsenopyrite decomposition should be accompanied by acidification, similar to pyrite decomposition processes. All the natural and mine-related examples described above have abundant coexisting calcite, so no net acidification is expected or observed. However, the laboratory experiments were done in the absence of calcite, and significant acidification was expected. Production of 750 ppm dissolved As, a representative experimental result (Table 2), is equivalent to 0.01 mol/l As, and this should produce ca. 0.1 mol/l hydrogen ions, equivalent to a pH of 1. In fact, the final pH of many of the solutions was little different from the initial pH, especially for the experiments done at low pH that resulted in the highest dissolved As (Fig. 3B). The most acidification that occurred resulted in change of only ca. 4 pH units. The chemical system in these simple experiments is clearly more complicated than that depicted in Eq. (1). At least part of this complication may be related to oxidation of As(III) to As(V).

Arsenopyrite coexisting with pyrite in near-surface water-saturated rocks is stable under Eh–pH conditions near to, but below, the upper stability limit for both pyrite and arsenopyrite (Fig. 4A,B). Water in equilibrium with arsenopyrite under these conditions surface should have ca. 0.01–0.1 ppm dissolved As (Fig. 4A and B, 5). Groundwater in contact with fresh mineralised rocks in the Otago Schist appears to be in chemical equilibrium with pyrite, as pyrite coats many joints (above). This groundwater has between 0.005 and 0.3 ppm dissolved As (Table 1), similar to that expected for equilibrium between arsenopyrite and water. Hence, chemical equilibrium between groundwater and arsenopyrite is plausible, based on the observations and calculations above. If this assertion is correct, maximum dissolved As concentrations in groundwaters should be predictable from pH and Eh of the waters, and concentrations of dissolved As should decline steeply with decreasing redox potential (Fig. 5). It will be difficult to test this assertion in highly reduced rocks as sampling access to these rocks, e.g., via drillholes, will allow oxidation and subsequent increase in dissolved As. This latter process may be occurring already in groundwater supply wells in basement rocks that have elevated dissolved As in many parts of the world (Smedley and Kinniburgh, 2002).

The revised stability range for arsenopyrite outlined above, combined with the field observations, has implications for predictions of long-term environmental stability of arsenopyrite-bearing mine tailings. Such tailings have commonly been considered to be an environmental threat even if the accompanying pyrite does not decompose, because of the perceived instability of arsenopyrite. However, our calculations and observations suggest that arsenopyrite should not decompose to any significant extent provided it is kept under moderately reducing conditions. This treatment has been successful for long-term storage of pyrite-bearing tailings, and generally involves permanent saturation with water to exclude oxygen (Elberling and Damgaard, 2001).

Acknowledgements

This study was funded by the New Zealand Foundation for Research, Science and Technology, and University of Otago. The research was facilitated with logistical help and access to geochemical data by GRD Macraes personnel, particularly Debbie Wilson. Debra Chappell set up the arsenopyrite experiments, Frank Ho assisted with analysis of the waters, and Amanda Black photographed Fig. 2A. **[EO]**

References

Barton, P.B., 1969. Thermodynamic study of the system Fe–As–S. Geochim. Cosmochim. Acta 33, 841–857.

Clough, D.M., Craw, D., 1989. Authigenic gold–marcasite association—evidence for nugget growth by chemical accretion in fluvial gravels, Southland, New Zealand. Econ. Geol. 84, 953–958.

Craw, D., Chappell, D.A., 1999. Evolution and sulphide mineral occurrences of an incipient nonmarine sedimentary basin, New Zealand. Sediment. Geol. 129, 37–50.

Craw, D., Pacheco, L., 2002. Mobilisation and bioavailability of arsenic around mesothermal gold deposits in a semiarid environment, Otago, New Zealand. Sci. World J. 2, 308–319.

Craw, D., Chappell, D., Nelson, M., Walrond, M., 1999. Consolidation and incipient oxidation of alkaline arsenopyrite-bearing mine tailings, Macraes Mine, New Zealand. Appl. Geochem. 14, 485–498.

Craw, D., Chappell, D., Reay, A., Walls, D., 2000. Mobilisation and attenuation of arsenic around gold mines, east Otago, New Zealand. N.Z. J. Geol. Geophys. 43, 373–383.

Elberling, B., Damgaard, L.R., 2001. Microscale measurements of oxygen diffusion and consumption in subaqueous sulfide tailings. Geochim. Cosmochim. Acta 65, 1897–1905.

Garrels, R.M., Christ, C.L., 1965. Solutions, Minerals, and Equilibria. Harper and Row Publ., New York.

Heinrich, C.A., Eadington, P.J., 1986. Thermodynamic predictions of the hydrothermal chemistry of arsenic and their significance for the paragenetic sequence of some cassiterite–arsenopyrite–base metal sulfide deposits. Econ. Geol. 81, 511–529.

Kretschmar, U., Scott, S.D., 1976. Phase relations involving arsenopyrite in the system Fe–As–S and their application. Can. Mineral. 14, 364–386.

Naumov, G.B., Ryzhenko, B.N., Khodakovsky, I.L., 1974. Handbook of Thermodynamic Data. U.S. Geological Survey, Reston, VA.

Nesbitt, H.W., Muir, I.J., 1998. Oxidation states and speciation of secondary products on pyrite and arsenopyrite reacted with mine waste waters and air. Mineral. Petrol. 62, 123–144.

Pokrovski, G.S., Gout, R., Zotov, A., Schott, J., Harrichoury, J.C., 1996. Thermodynamic properties and stoichiometry of the arsenic(III) hydroxide complexes at hydrothermal conditions. Geochim. Cosmochim. Acta 60, 737–749.

Pokrovski, G.S., Kara, S., Roux, J., 2002. Stability and solubility of arsenopyrite, FeAsS, in crustal fluids. Geochim. Cosmochim. Acta 66, 2361–2378.

Richardson, S., Vaughan, D.J., 1989. Arsenopyrite: a spectroscopic investigation of altered surfaces. Mineral. Mag. 53, 223–229.

Rittle, K.A., Drever, J.I., Colberg, P.J.S., 1995. Precipitation of arsenic during bacterial sulfate reduction. Geomicrobiol. J. 13, 1–11.

Shock, E.L., Helgeson, H.C., 1988. Calculation of the thermodynamic and transport properties of aqueous species at high pressure and temperature: correlation algorithm for ionic species and equation of state predictions to 5 kb and 1000°C. Geochim. Cosmochim. Acta 52, 2009–2036.

Smedley, P.L., Kinniburgh, D.G., 2002. A review of the source, behaviour and distribution of arsenic in natural waters. Appl. Geochem. 17, 517–568.

Smedley, P.L., Edmunds, W.M., Pelig-Ba, K.B., 1996. Mobility of arsenic in groundwater in the Obuasi gold-mining area of Ghana: some implications for human health. Spec. Publ. - Geol. Soc. Lond. 113, 163–181.

Vink, B.W., 1996. Stability relations of antimony and arsenic compounds in the light of revised and extended Eh–pH diagrams. Chem. Geol. 130, 21–30.

Wagman, D.D., Evans, W.H., Parker, V.B., Schumm, R.H., Halow, I., Bailey, S.M., Churney, K.L., Nuttall, R.L., 1982. The NBS tables of chemical thermodynamic properties. J. Phys. Chem. Ref. Data 11 (Suppl. 2).

Webster, J.G., 1990. The solubility of As_2S_3 and speciation of As in dilute sulfide-bearing fluids at 25 and 90°C. Geochim. Cosmochim. Acta 54, 1009–1017.

Williams, G.J., 1974. Economic geology of New Zealand. Aust. Inst. Min. Metall. Monogr., vol. 4. 490 pp.